Supporting Information

Boosting the Zn-ion transfer kinetics to stabilize the Zn metal interface for high-performance rechargeable Zn-ion batteries

Lin Hong, Xiuming Wu, Chao Ma, Wei Huang,* Yongfeng Zhou, Kai-Xue Wang,* Jie-Sheng Chen

School of Chemistry and Chemical Engineering, State Key Laboratory of Metal Matrix Composites, Shanghai Jiao Tong University, 800 Dongchuan Road, Shanghai 200240, P. R. China.

E-mail: hw66@sjtu.edu.cn (WH); k.wang@sjtu.edu.cn (KXW)

Experimental Section

Materials: Montmorillonite (> 99.9%), $ZnCl_2$ (> 99.0%), $MnSO_4$ (> 99.0%), $KMnO_4$ (> 99.0%), $ZnSO_4$ (> 99.0%) were purchased from Sigma-Aldrich Chemical Co. All other reagents were analytical grade and used directly without further purification. Deionized water was used to prepare all aqueous electrolytes.

Preparation of Zn-Mont: In a typical procedure, 2.0 g of montmorillonite was acidactivated with 150 mL of HCl (0.01 M) at 60 °C for 3 h under magnetic stirring. The acid-activated montmorillonite was centrifuged and washed thoroughly with distilled water several times. Then, the obtained montmorillonite was dried at 70 °C for 24 h under vacuum, and mechanically ground into ultrafine powder. Subsequently, the acid-activated montmorillonite was added into 150 mL of 1.0 M $ZnCl_2$ solution, followed by stirring at 100 °C for 30 min under reflux and then 70 °C for 8 h[1]. The Zn-ion loaded montmorillonite was collected by centrifugation (7000 rpm, 10 min) of the reaction mixture, washing repeatedly with distilled water, vacuum drying (70 °C, 24 h) and mechanical grinding. The

Zn-ion intercalated montmorillonite was denoted as Zn-Mont and the untreated montmorillonite as Ca-Mont.

Preparation of Zn@Zn-Mont: Zn-Mont and PVDF were mixed with a weight ratio of 8:2 and formed slurry by adding NMP dispersant. The slurry was coated onto Zn foil (30 μm) and dried at 70 °C for 24 h under vacuum. For comparison, Zn@Ca-Mont was also prepared by replacing Zn-Mont with Ca-Mont.

Preparation of MnO_2: MnO_2 powders were prepared by a hydrothermal method according to the previous work[2]. Briefly, 2.0 mL of H_2SO_4 solution (0.5 M) was added into 90 mL of $MnSO_4$ solution (0.003 M) under magnetically stirring until a transport solution was obtained. Then, 20 mL of $KMnO_4$ solution (0.1 M) was added into the above solution drop by drop. After further stirring for 2 h, the mixture was transferred into a Teflonlined autoclave and maintained at 120 °C for 12 h. Finally, the resulting product was collected by centrifugation, washed thoroughly with deionized water, and dried at 70 °C for 24 h under vacuum.

Materials characterizations: Powder X-ray diffraction (XRD) patterns were collected by a Rigaku Mini Flex 600 diffractometer using Cu Kα-radiation (λ= 1.5418). The morphology of the samples was collected on a field emission scanning electron microscope (SEM, Nova NanoSEM 450) equipped with an energy dispersive X-ray spectrometer (EDS). XPS measurements was conducted on AXIS Ultra DLD X-ray photoelectron spectrometer. The spinning disk confocal microscopy (SDCM) images have been collected on Zeiss Smartproof 5 microscope. The specific surface areas of samples were analyzed by Brunauere-Emmette-Teller (BET) method (micromeritics ASAP 2020). The in situ optical visualization observations of Zn plating/stripping behavior were performed on an optical microscope (LEICA DM 4000).

Electrochemical measurements: CR2032-type coin Zn-Zn symmetric cells were assembled with two identical electrodes of bare Zn, Zn@Ca-Mont or Zn@Zn-Mont (diameter: 12 mm, thickness: 30 μm), 2.0 M $ZnSO_4$ electrolyte and glass fiber separators. To analyze the coulombic efficiency of Zn deposition/dissolution, Cu foil, Cu@Ca-Mont, or Cu@Zn-Mont was used as working electrode, and Zn foil was employed as counter electrode. The cathode electrodes were composed of MnO_2, conductive carbon black and polyvinylidene fluoride (PVDF) at a weight ratio of 8:1:1, using NMP as solvent. The resulting slurry was coated on disc-shaped stainless steel meshes (Φ = 12 mm) and then dried in a vacuum oven at 80 °C for 12 h. The cathode and anode electrodes were separated by glass fiber separators (Φ = 19 mm). 2.0 M $ZnSO_4$ + 0.1 M $MnSO_4$ aqueous solution was used as electrolyte for all coin cells in this work, which were assembled in the air atmosphere. All the galvanostatic charge/discharge tests were conducted on a Neware battery testing system. CV, EIS, and corrosion tests were tested using an electrochemical workstation (CHI760E, China).

Computational Method: Density functional theory (DFT) calculations were carried out using projector-augmented wave (PAW) method as implemented in Vienna ab initio simulation package (VASP) [3-5]. A generalized gradient approximation (GGA) of Perdew-Burke-Ernzerhof (PBE) functional was employed to describe the exchange-correlation interaction [6]. The DFT-D3 method was also adopted to evaluate the van der Waals interactions [7]. To ensure the accuracy of the calculated results, the energy cutoff was set to 520 eV and the Brillouin zone was sampled by 5×3×5 Monkhorst-Pack k-points mesh in all calculations. The structures were relaxed until the forces and total energy on all atoms were converged to less than 0.05 eV $Å^{-1}$ and 1×10^{-5} eV. Diffusion barriers for Zn hopping between adjacent interstitial sites in the interlayer are calculated using the climbing-image nudged elastic band (CI-NEB) method [8].

Table S1 Performance comparison of symmetric cell and full cell for this work with recently reported cells.

	Symmetric cell performance			Full cell performance				
Electrode	**Current (mA/cm^2)**	**Capacity (mAh/cm^2)**	**Life (h)**	**Cathode**	**Current**	**Capacity (mAh/g)**	**Cycle**	**Reference**
Zn@Zn-Mont	**2**	**1**	**700**	**MnO_2**	**2 C**	**197.5**	**1000**	**This work**
ZF@F-TiO_2	1	1	460	MnO_2	1 A/g	80	300	9
$CaCO_3$ coated Zn	2	0.1	80	MnO_2	1 A/g	175	1000	10
Zn@ZIF-8	1	1	50	-	-	-	-	11
Zn/CNT	2	2	200	MnO_2	20 mA/cm^2	165	1000	12
Zn@CFs	1	1	160	MnO_2	1 C	207	140	13
NTP@Zn	1	1	250	MnO_2	5 C	128	600	14
MZn-60	0.2	0.2	800	MnO_2	1 A/g	205	500	15
CM@CuO@Zn	1	1	340	MnO2	5 A/g	140	900	16
Zn/C_3N_4	2	2	500	-	-	-	-	17
r-Zn	1	0.2	400	-	-	-	-	18

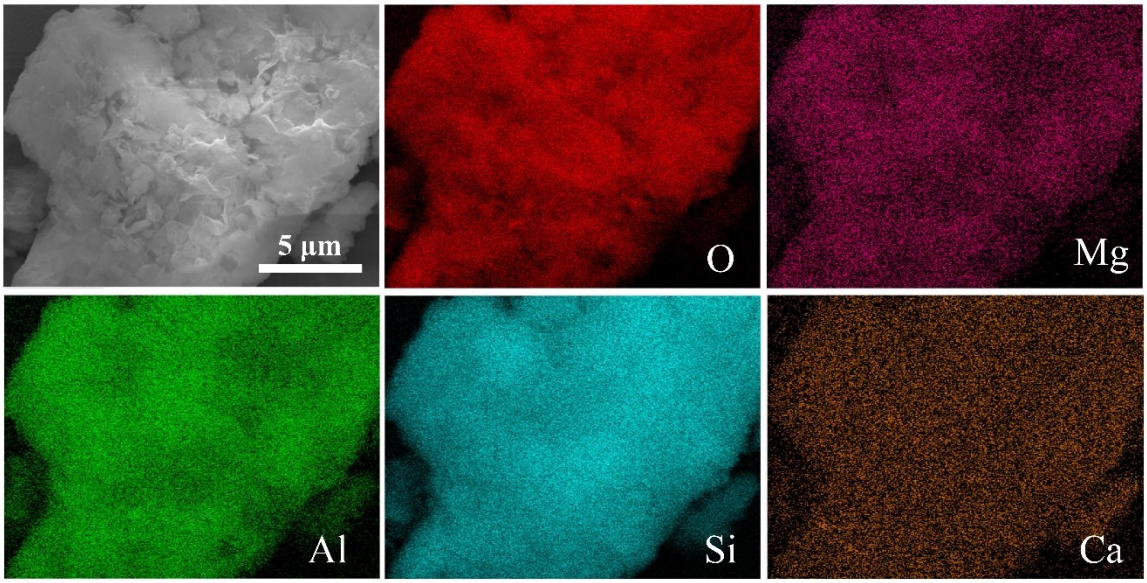

Figure S1 EDS elemental mapping images of Ca-Mont powder.

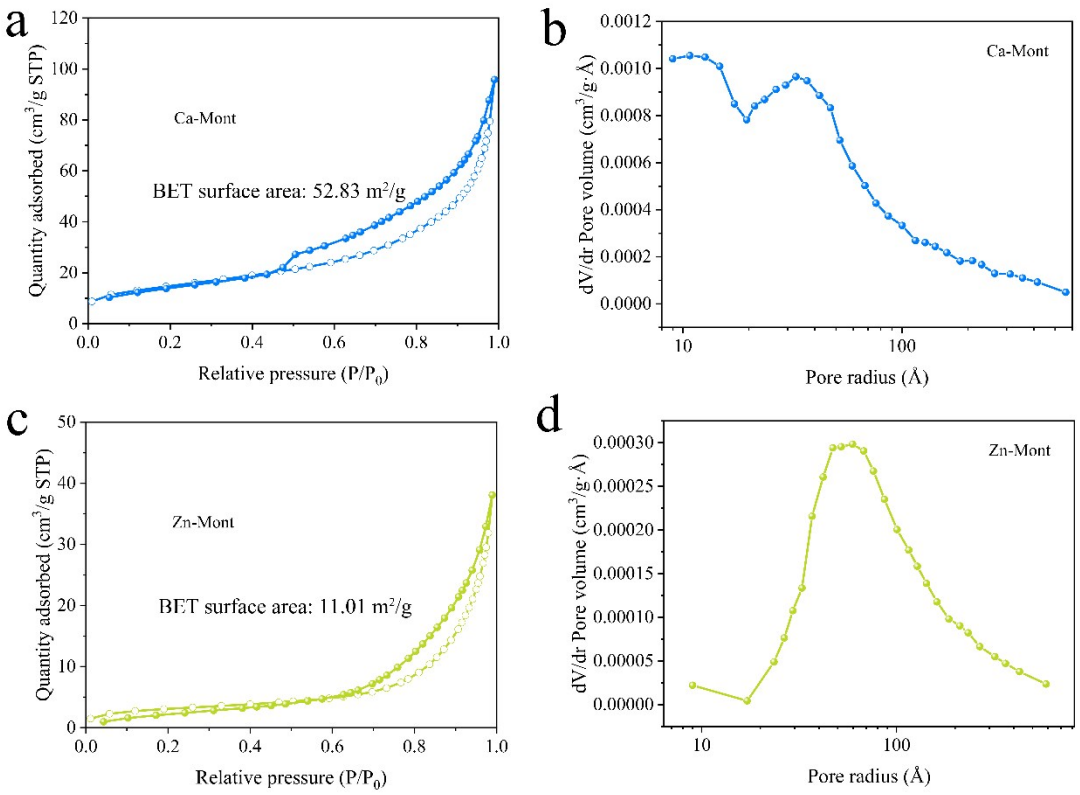

Figure S2 (a, c) Nitrogen adsorption/desorption isotherms and (b, d) pore size distributions of (a, b) Ca-Mont and (c, d) Zn-Mont.

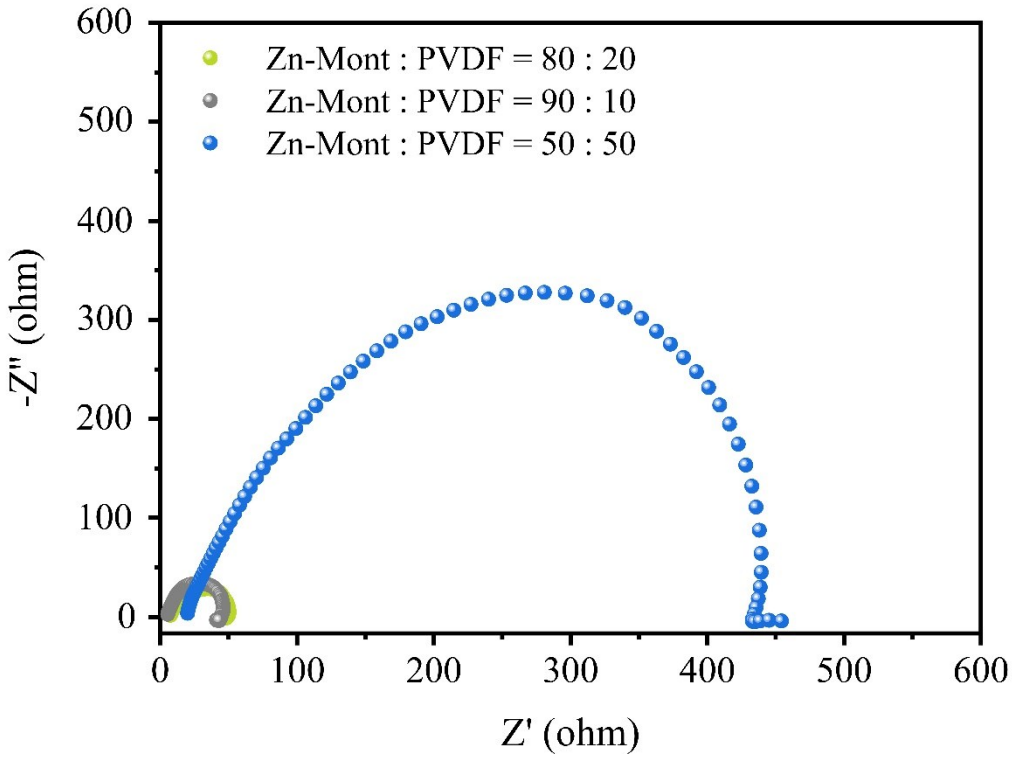

Figure S3 Nyquist plots of symmetric cells using Zn@Zn-Mont electrodes with different Zn-Mont/PVDF ratio (90:10, 80:20, and 50:50).

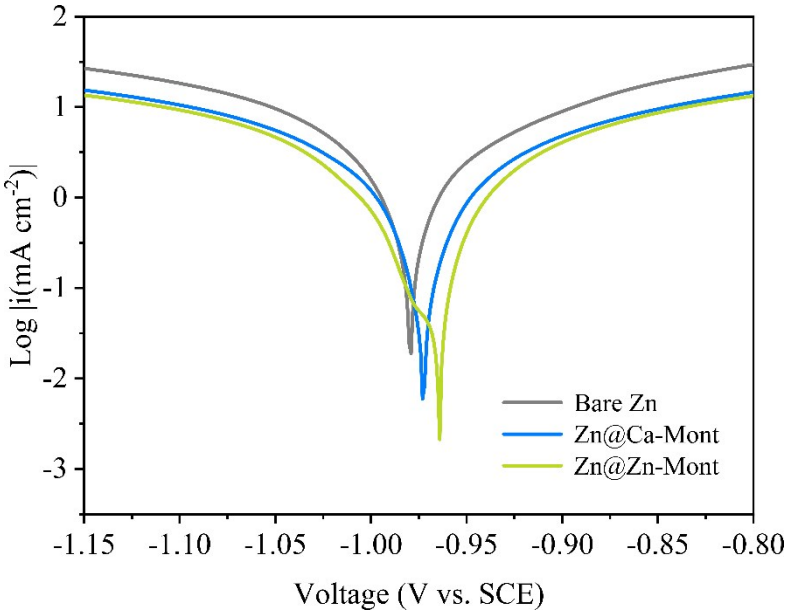

Figure S4 Corrosion curves of the bare Zn, Zn@Ca-Mont, and Zn@Zn-Mont anodes.

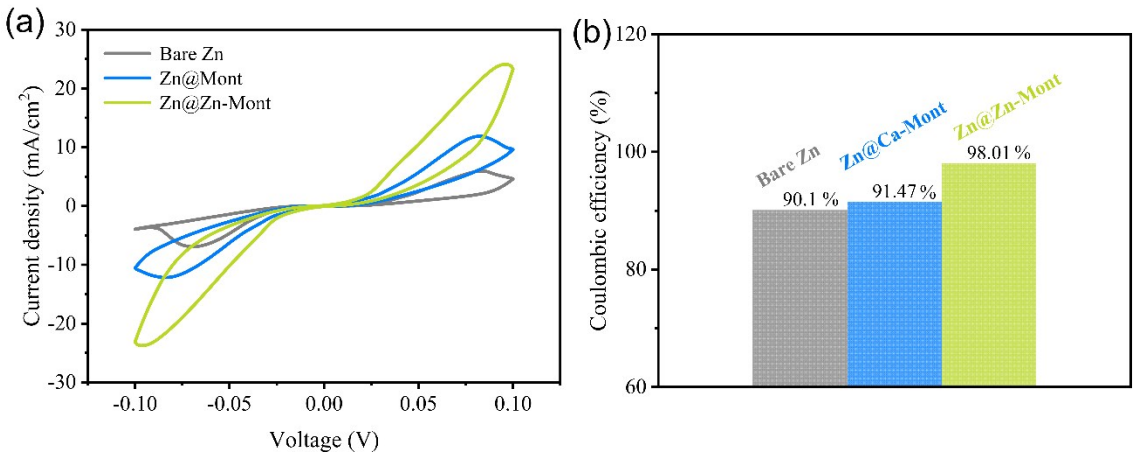

Figure S5 (a) CV curves of Zn||Zn symmetric cells measured at 0.1 mV s^{-1}, and (b) corresponding Coulombic efficiency.

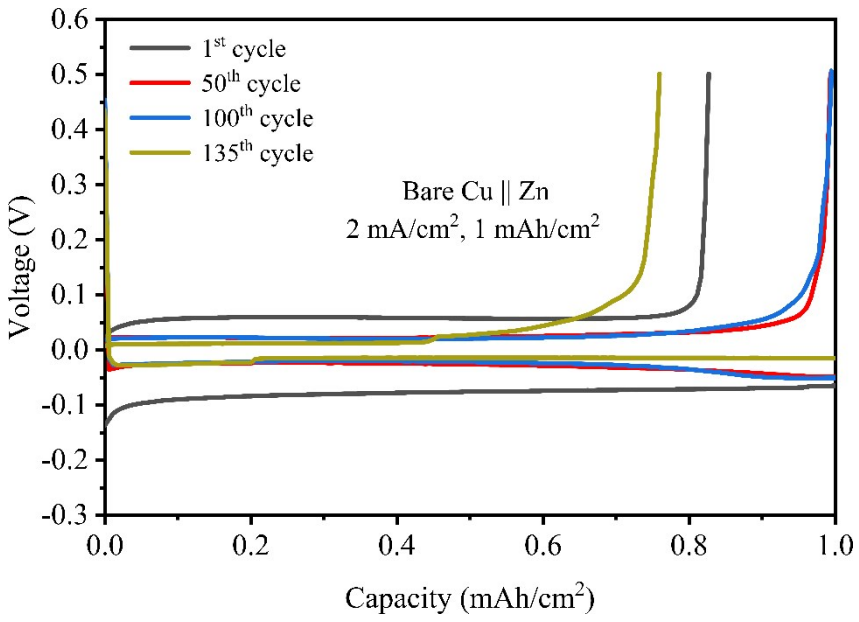

Figure S6 Voltage profiles of the bare Cu || Zn at 2.0 mA/cm^2 with 1.0 mAh/cm^2.

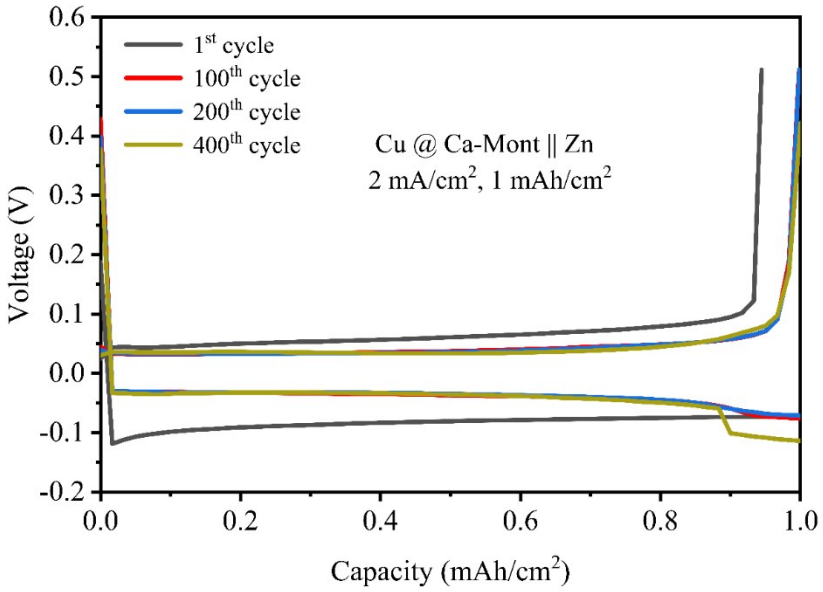

Figure S7 Voltage profiles of the Cu@Ca-Mont || Zn at 2.0 mA/cm^2 with 1.0 mAh/cm^2.

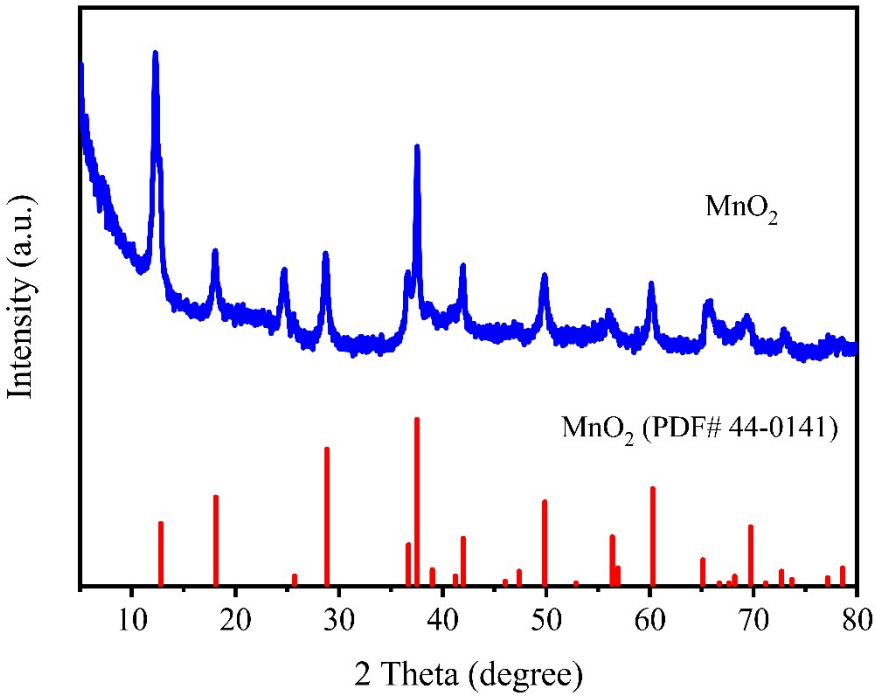

Figure S8 XRD pattern of MnO_2.

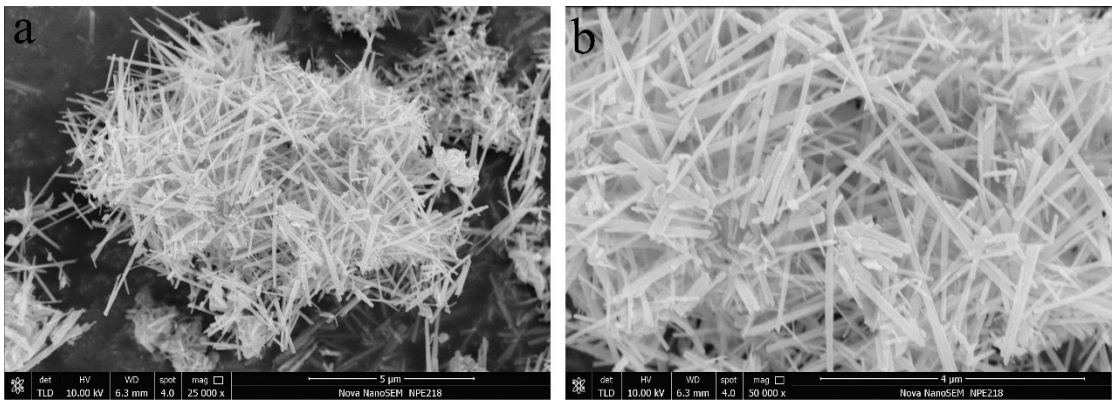

Figure S9 FE SEM images of MnO_2.

References

[1] A. Roy, M. Joshi and B. S. Butola, *J. Cleaner Prod.*, 2019, **212**, 1518-1525.

[2] H. Pan, Y. Shao, P. Yan, Y. Cheng, K. S. Han, Z. Nie, C. Wang, J. Yang, X. Li, P. Bhattacharya, K. T. Mueller, J. Liu, *Nat. Energy* 2016, **1**, 16039.

[3] Kresse G., Hafner J., *Phys. Rev. B.*, 1993, **47**, 558-561.

[4] Kresse G., Furthmüller J., *Phys. Rev. B.*, 1996, **54**, 11169-11186.

[5] Blöchl P. E., *Phys. Rev. B.*, 1994, **50**, 17953-17979.

[6] Perdew J. P., Burke K., Ernzerhof, M., *Phys. Rev. Lett.*, 1996, **77**, 3865-3868.

[7] S. Grimme, J. Antony, S. Ehrlich, and S. Krieg, *J. Chem. Phys.*, 2010, **132**, 154104.

[8] G. Henkelman, H. Jonsson, *J. Chem. Phys.*,2000, **113**, 9978-9985.

[9] Q. Zhang, J. Luan, X. Huang, Q. Wang, D. Sun, Y. Tang, X. Ji and H. Wang, *Nat. Commun.*, 2020, **11**, 3961.

[10] L. Kang, M. Cui, F. Jiang, Y. Gao, H. Luo, J. Liu, W. Liang and C. Zhi, *Adv. Energy Mater.*, 2018, **8**, 1801090.

[11] Z. Wang, J. Huang, Z. Guo, X. Dong, Y. Liu, Y. Wang and Y. Xia, *Joule*, 2019, **3**, 1289-1300.

[12] Y. Zeng, X. Zhang, R. Qin, X. Liu, P. Fang, D. Zheng, Y. Tong and X. Lu, *Adv.*

Mater., 2019, **31**, 1903675.

[13] W. Dong, J.-L. Shi, T.-S. Wang, Y.-X. Yin, C.-R. Wang and Y.-G. Guo, *RSC Adv.*, 2018, **8**, 19157-19163.

[14] M. Liu, J. Cai, H. Ao, Z. Hou, Y. Zhu and Y. Qian, *Adv. Funct. Mater.*, 2020, **30**, 2004885.

[15] N. Zhang, S. Huang, Z. Yuan, J. Zhu, Z. Zhao and Z. Niu, *Angew. Chem., Int. Ed.*, 2021, **60**, 2861-2865.

[16] Q. Zhang, J. Luan, X. Huang, L. Zhu, Y. Tang, X. Ji and H. Wang, *Small*, 2020, **16**, 2000929.

[17] P. Liu, Z. Zhang, R. Hao, Y. Huang, W. Liu, Y. Tan, P. Li, J. Yan and K. Liu, *Chem. Eng. J.*, 2021, **403**, 126425.

[18] J. Wang, Z. Cai, R. Xiao, Y. Ou, R. Zhan, Z. Yuan and Y. Sun, *ACS Appl. Mater. Interfaces*, 2020, **12**, 23028-23034.